Concentration distribution in solution crystal growth: effect of moving interface conditions

W. Wang*, W.R. Hu

Institute of Mechanics, Chinese Academy of Sciences, Beijing 100 080, People's Republic of China

Abstract

The linear diffusion–reaction theory with finite interface kinetics is employed to describe the dissolution and the growth processes. The results show that it is imperative to consider the effect of the moving interfaces on the concentration distribution at the growth interface for some cases. For small aspect ratio and small gravity magnitude, the dissolution and the growth interfaces must be treated as the moving boundaries within an angle range of $0° < \gamma < 50°$ in this work. For large aspect ratio or large gravity magnitude, the effect of the moving interfaces on the concentration distribution at the growth interface can be neglected except for $\gamma < -50°$. © 1999 Published by Elsevier Science B.V. All rights reserved.

Keywords: Concentration distribution; Interface conditions

1. Introduction

The structure and properties of the crystal products grown from solution are significantly influenced by the concentration distribution adjacent to the crystal interface. Xu et al. [1–3] have studied the crystal growth from solution using a two dimensional cuboidal model, and revealed the characteristics of solution crystal growth under microgravity. They simplified the crystal dissolution and growth processes as the pure diffusion processes. In fact, the solution in contact with the growth crystal interface is non-uniformly supersaturated [4], and the buoyancy-driven convection influences the non-uniformity supersaturation. Wang and Hu [5,6] modified their model by employing the linear diffusion–reaction theory with finite interface kinetics, and discussed the effect of the microgravity-driven convection on the solution concentration distribution at the growth interface. Since the kinetic coefficient for the dissolution process was unavailable, Sun et al. [7] had to employ the same value as used in the growth process. Considering generally that a substance dissolves at a faster rate than it crystallizes, Wang and Hu [5,6] retained the pure diffusion dissolution process under the same conditions of temperature and concentration. Careful attention must be shown to the

* Corresponding author. Tel.: +86 010 62545533 3026; fax: +86 010 62561284; e-mail: wwei@nml.imech.ac.cn.

effect of the concentration boundary at the dissolution interface on the concentration distribution at the growth interface. Hu and You [8] numerically studied the float zone crystal growth, and pointed out that the change of the concentration boundary conditions at the melt interface may result in the change of the concentration distribution at the crystal interface. Therefore, in order to investigate the effect of the concentration boundary conditions at the dissolution interface on the concentration distribution near the growth interface, the diffusion-reaction theory with finite interface kinetics must be employed to describe the dissolution process. Strictly speaking, the crystal dissolution and crystallization gives rise to a moving boundary problem. In previous papers [5–7,9], both the growth rate and the dissolution rate are much lower than the typical convection velocity, the actual moving boundaries were simplified as fixed interfaces. Based on the mass balance relationship between growth and dissolution, Wang and Hu [10] recently further improved the previous model.

In the present paper, the diffusion–reaction theory with finite kinetics was employed to describe both dissolution and growth processes, and the growth and dissolution interfaces were regarded as the moving interfaces. In the following section the model and the numerical scheme are described. In Section 3 we present and discuss the results. A summary is given in Section 4.

2. Mathematical model and numerical scheme

Similar to the simplification in previous papers [5,6,10], this study adopts a generic model, in which the sodium chlorate ($NaClO_3$) crystal grows in a two dimensional rectangular enclosure filled with sodium chlorate aqueous solution after sufficient time in the steady microgravity background g, as shown in Fig. 1, and γ is the gravity orientation angle to the $-Y^*$ axis. Two vertical walls of the cavity are made of the $NaClO_3$ seed crystal and the $NaClO_3$ sources, respectively. The dissolution interface is maintained at a higher temperature T_S^* compared to T_C^* at the dissolution interface. The top and bottom walls are impermeable and adiabatic. The dimension in Z^* direction is large
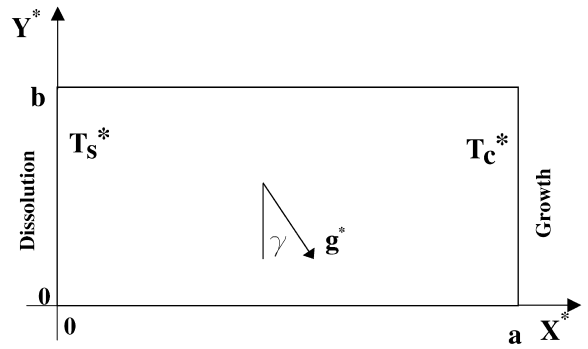

Fig. 1. The schematic diagram of generic model.

enough, so the two dimensional model is used. For the quasi-steady state crystal growth, the assumption of equal the growth velocity and the dissolution velocity is implicit. The aspect ratio of the cavity is defined as $\lambda = b/a$ of height b and width a. The Boussinesq approximation is applied. In the relative coordinate system, which is fixed at the dissolution interface, the two dimensional steady-state governing equations for conservation of mass, momentum, energy, and concentration in non-dimensional form are given as follows:

$$\frac{1}{Pr}\nabla\cdot(V\omega) = \nabla^2\omega + Ra_c\left(\frac{\partial\phi}{\partial X}\cos\gamma + \frac{\partial\phi}{\partial Y}\sin\gamma\right)$$

$$- Ra_t\left(\frac{\partial\vartheta}{\partial X}\cos\gamma + \frac{\partial\vartheta}{\partial Y}\sin\gamma\right),$$

$$\nabla\cdot(V\phi) = \frac{1}{Le}\nabla^2\phi,$$

$$\nabla\cdot(V\vartheta) = \nabla^2\vartheta,$$

$$\nabla^2\psi = \omega, \tag{2.1}$$

where, $V = (V_X e_X + V_Y e_Y)$, ψ, ω, ϑ and ϕ are, respectively, the non-dimensional velocity vector, stream function, vorticity, temperature, and concentration. The dimensionless variables and parameters are defined as

$$\lambda = \frac{b}{a}, \ X = \frac{X^*}{a}, \ Y = \frac{Y^*}{a}, \ V_X = \frac{V_{X^*}^*}{V_0}, \ V_Y = \frac{V_{Y^*}^*}{V_0},$$

$$\psi = \frac{\psi^*}{V_0 a}, \ \omega = \frac{\omega^* a}{V_0}, \ \phi = \frac{C^* - C_C^*}{C_S^* - C_C^*}, \ \vartheta = \frac{T^* - T_C^*}{T_S^* - T_C^*}.$$

$$\tag{2.2}$$

where the starred quantities denote dimensional values, C_S^* and C_C^* are the equilibrium solubility at T_S^* and T_C^*, respectively, $V_0 = \kappa/a$ is a typical velocity, κ the thermal diffusivity ν the kinematic viscosity and D the solution diffusion coefficient.

$\mathrm{Ra_t}$, $\mathrm{Ra_c}$, Pr and Le are, respectively, the thermal Rayleigh number, solute Rayleigh number, Prandtl number and Lewis number, which are defined as follows:

$$\mathrm{Ra_t} = \frac{\beta a^3 g g_0 (T_S^* - T_C^*)}{\nu\kappa}, \quad \mathrm{Ra_c} = \frac{\alpha a^3 g g_0 (C_S^* - C_C^*)}{\nu\kappa},$$

$$\mathrm{Pr} = \frac{\nu}{\kappa}, \quad \mathrm{Le} = \frac{\kappa}{D}, \tag{2.3}$$

where g is the terrestrial gravity acceleration, g_0 the ratio of local gravity to earth's gravity, $\alpha = 1/\rho^*(\partial\rho^*/\partial C^*)$ is the solutal expansion coefficient and $\beta = -1/\rho^*(\partial\rho^*/\partial T^*)$ the thermal expansion coefficient.

With the linear diffusion–reaction theory, the non-dimensional boundary conditions associated with this model are

$$X = 0: \quad V_X = V_Y = 0, \ \vartheta = 1, \quad \frac{\partial\phi}{\partial X} = K_S(\phi - 1),$$

$$X = 1: \quad V_X = V_Y = 0, \ \vartheta = 0, \quad \frac{\partial\phi}{\partial X} = -K_C\phi,$$

$$Y = 0: \quad V_X = AV_{ac}, V_Y = 0, \quad \frac{\partial\vartheta}{\partial Y} = \frac{\partial\phi}{\partial Y} = 0,$$

$$Y = \lambda: \quad V_X = AV_{ac}, V_Y = 0, \quad \frac{\partial'}{\partial Y} = \frac{\partial\phi}{\partial Y} = 0. \tag{2.4}$$

where $K_C = k_c^* a/D$ and $K_S = k_s^* a/D$ are the non-dimensional growth and dissolution interface kinetics, respectively. K_C can be calculated with the known dimensional growth kinetic coefficient k_c^* [11]. But for the simpler model in which the pure diffusion dissolution process and the fixed interfaces are assumed, the boundary conditions are simplified by adopting $K_S \to \infty$ and $V_{ac} = 0$.

In Eq. (2.4) K_S must be solved using the following mass balance relationship between growth and dissolution for the steady model:

$$M_C = M_S, \tag{2.5}$$

$$M_C = \rho_{cry} V_{ac}$$

$$= -\rho_{cry} \int_0^\lambda \left.\frac{\partial\phi}{\partial X}\right|_C \mathrm{d}Y$$

$$= \rho_{cry} \int_0^\lambda K_C \phi_C \, \mathrm{d}Y,$$

$$M_S = \rho_{cry} V_{ac}$$

$$= -\rho_{cry} \int_0^\lambda \left.\frac{\partial\phi}{\partial X}\right|_S \mathrm{d}Y$$

$$= \rho_{cry} \int_0^\lambda K_S (1 - \phi_s) \, \mathrm{d}Y,$$

where M_C and M_S are the solute flux at growth interface and dissolution interface, respectively. ρ_{cry} is the non-dimensional crystal density. The crystal density difference between the seed and the source is neglected in this work. $V_{ac} = -\int_0^\lambda (\partial\phi/\partial X)|_C \, \mathrm{d}Y$ is the non-dimensional crystal average growth velocity which must be iteratively solved. Constant $A = D(C_S^* - C_C^*)/\rho_{cry}^*\kappa$ arises from the difference between the typical velocity of fluid flow and the typical crystal growth velocity.

Eq. (2.1) associated with boundary conditions expressed by Eq. (2.4) is numerically solved using the finite difference method. The numerical scheme used in this work is similar to the previous paper [10]. The simulation process is presented here again. The calculation begins with the initial values of unknown K_S and V_{ac}. In order to obtain the accurate results, two successive convergence criterions are employed. The first one is that the maximums relative error in the dependent variables is less than 10^{-6} between two successive iterations for a fixed K_S. V_{ac} can be solved in each iteration. After the first criterion is achieved, the mass balance relationship between growth and dissolution must be checked. The study requires that the relative error in the solute flux is less than 10^{-2} in this work. If the second requirement fails, the first circulation calculation continues with a new K_S obtained by Eq. (2.5).

3. Results and discussion

In this paper, the same thermophysical properties and the operating conditions of the sodium chlorate solution as in previous papers [5,6,10] are used, thus the relationship $Ra_t = 0.385\ Ra_c = 5.175 \times 10^7 g_0$ remains. Since the solution flow is the concentration dominated, the convection driven by both thermal gradient and concentration gradient must be considered. Ra_t stands for the magnitude of gravity. Because the effects of moving interfaces and the concentration boundary conditions at dissolution interface can be certainly distinguished from the given results, this work does not separately present the two effects.

In the resulting figures, case 1 represents the new model, in which the dissolution process is also described by the diffusion-reaction theory and the effect of moving interfaces are considered; case 2 stands for the simple model, in which the dissolution process is described by the pure diffusion process and the interfaces are assumed as fixed boundaries. Figs. 2 and 3 show the concentration profiles at the growth and the dissolution interfaces, respectively. For $\lambda = 0.2$, $Ra_t = 1000$, $\gamma = -30°$, Fig. 3a illustrates that the concentration at the dissolution interface is non-uniform, but the value is very close to the solubility, the maximal

relative difference is not larger than 0.05%, and the non-uniformity is small enough to be neglected for case 1, which means that the dissolution process is almost controlled by the diffusion process. However, Fig. 2a shows that the concentration at the growth interface of case 1 is obviously larger than that of case 2. According to the above results, it is impossible to absolutely conclude that the concentration boundary conditions at the dissolution interface have nothing to do with the concentration distribution at the growth interface, but it is an affirmation that the moving interfaces are the predominant factors. For comparison, Fig. 2b and 3b show that for the case of $\lambda = 0.2$, $Ra_t = 10\,000$, $\gamma = 30°$, the difference of ϕ_S between cases 1 and 2 is obvious, interestingly, ϕ_c of case 1 is very close to that of case 2. Thus, it is not hard for us to conclude that the effect of the concentration boundary conditions is limited, but the effect of moving interfaces on the concentration distribution at the growth interface is obvious in some cases. We confer that the reason why ϕ_c of case 1 is very close to that of case 2 for large Ra_t is that for $\lambda = 0.2$, $Ra_t = 10\,000$, $\gamma = 30°$ the convection velocity is much faster than the crystal growth velocity. Thus, the effect of the moving interfaces on the concentration distribution relatively decreases.
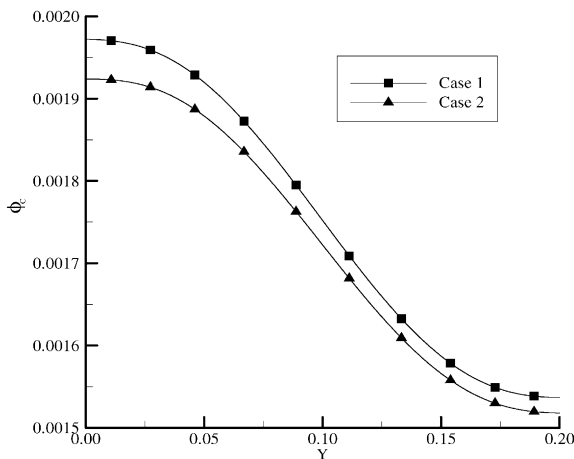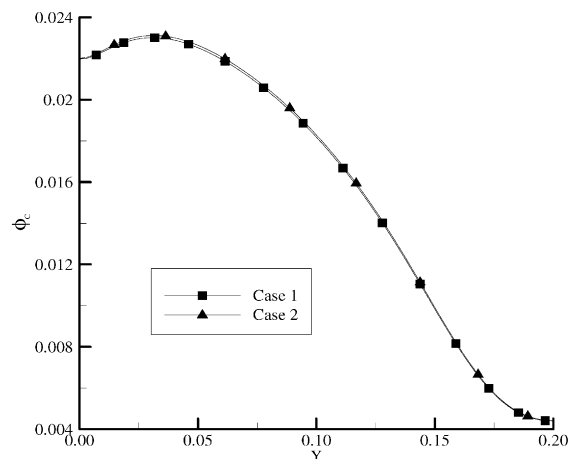
(a). $\lambda = 0.2, Ra_t = 1000, \gamma = -30°$ (b). $\lambda = 0.2, Ra_t = 10000, \gamma = 30°$

Fig. 2. Concentration profiles at the growth interface.
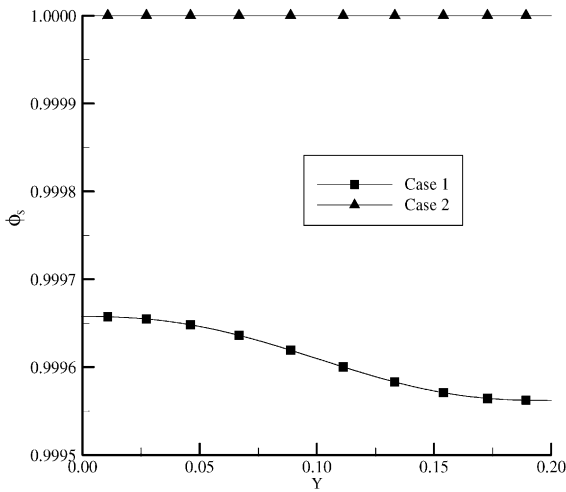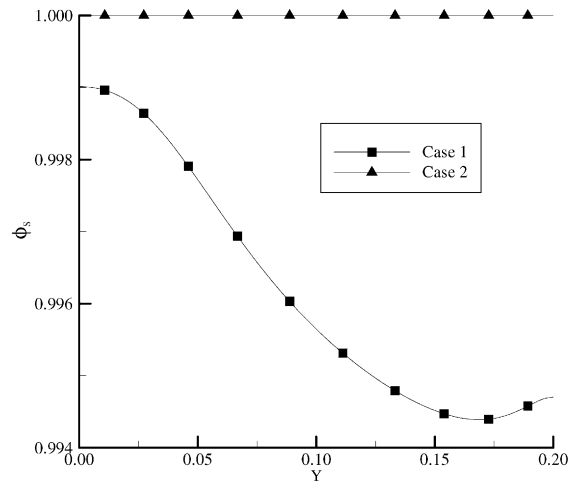
(a). $\lambda = 0.2, Ra_t = 1000, \gamma = -30°$

(b). $\lambda = 0.2, Ra_t = 10000, \gamma = 30°$

Fig. 3. Concentration profiles at the dissolution interface.

In order to approve this presumption, Fig. 4a, 4b and Fig. 5 illustrate the non-dimensional maximum solution velocity V_{max}, the interfaces moving velocity $V_B = AV_{ac}$ and the ratio V_B/V_{max} versus the gravity orientation γ, respectively. From Fig. 4a it can be seen that V_{max} increases as Ra_t or λ increases, and the change is very different at various orientations. For example, the change is very limited for $\gamma < -50°$, but obvious for $\gamma \geqslant -50°$, especially for large positive orientations. For $\lambda = 0.2$, $Ra_t = 10\,000$ and $\lambda = 0.4$, $Ra_t = 1000$, it is can be also see that V_{max} increases as γ increases, and for $\gamma < -50°$ the amplitude of V_{max} is small, but for $\gamma \geqslant -50°$ V_{max} almost linearly increases until γ reaches to 70°, after which the change tends to be gradual. For $\lambda = 0.2$, $Ra_t = 1000$, the change of V_{max} with γ is limited. Fig. 4b shows that V_B is much smaller than V_{max}, and the change of V_B with Ra_t and λ is almost similar to that of V_{max}. For $\lambda = 0.2$, $Ra_t = 1000$, the change of V_B with γ is also limited, but for $\lambda = 0.2$, $Ra_t = 10\,000$ and $\lambda = 0.4$, $Ra_t = 1000$ V_B slowly increases as γ increases when $\gamma < -50°$; when $-50° \leqslant \gamma \leqslant 50°$, V_B significantly increases; when $\gamma > 50°$, V_B decreases. The reason for the last behavior, the decreases of V_B when $\gamma > 50°$, is that the fluid vortex moves upward along the growth interface, which then results in the

local concentration gradient, $-\partial\phi/\partial X$, at the lower part of the growth interface significantly decreases as illustrated in Fig. 6.

Fig. 5 clearly illustrates the effect of the moving interfaces on the crystal growth environment. It is obvious that V_B/V_{max} decreases as Ra_t or λ increases. Similarly, the change of V_B/V_{max} is different at various orientations. For example, V_B/V_{max} significantly decreases as Ra_t or λ increases for $\gamma < -50°$, but weakly decreases for $\gamma > 50°$. For fixed Ra_t and λ, the change of V_B/V_{max} with γ is more obvious. For the three cases considered, as γ increases, V_B/V_{max} significantly decreases when $\gamma < -50°$, after then, V_B/V_{max} changes smoothly. When $\gamma > 50°$, V_B/V_{max} slightly increases only for $\lambda = 0.2$, $Ra_t = 1000$.

To date, we are sure that the effect of the moving interfaces on the concentration distribution at the growth interface must be considered for the cases of small Ra_t and λ which means that the dissolution and growth interfaces must be treated as the moving boundaries so as to obtain the accuracy concentration distribution at the growth interface, except for only in a limited range of γ (e.g., $0° \leqslant \gamma \leqslant 50°$ for $\lambda = 0.2$, $Ra_t = 1000$). For large Ra_t or large λ, the decision to consider these effects depends on the gravity orientation: when γ is small (e.g., $\gamma < -50°$

(a)

$A - \lambda = 0.2, Ra_t = 1000; B - \lambda = 0.2, Ra_t = 10000; C - \lambda = 0.4, Ra_t = 1000$

(b)
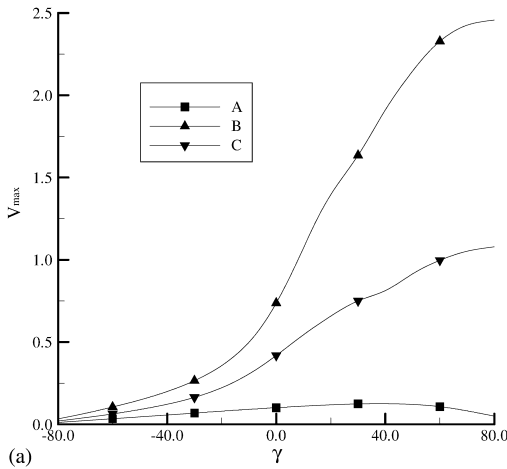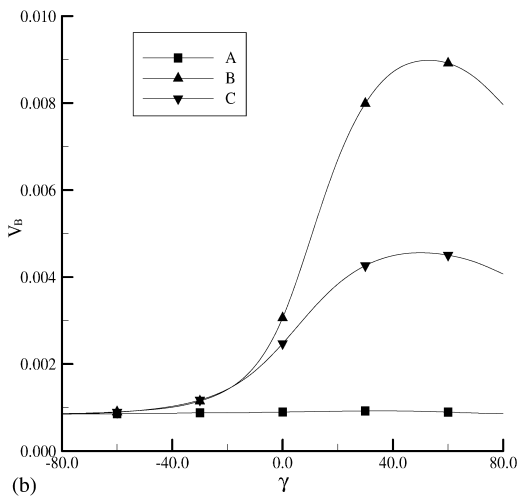
$-\lambda = 0.2, Ra_t = 1000; B - \lambda = 0.2, Ra_t = 10000; C - \lambda = 0.4, Ra_t = 1000$

Fig. 4. Dimensionless maximum solution velocity depending on gravity orientation (a) and dimensionless interfaces moving velocity depending on gravity orientation (b).

in this work), the effect must be considered; when γ is large (e.g., $\gamma \geqslant -50°$), the simple treatment can give the accuracy concentration distribution at the growth interface.
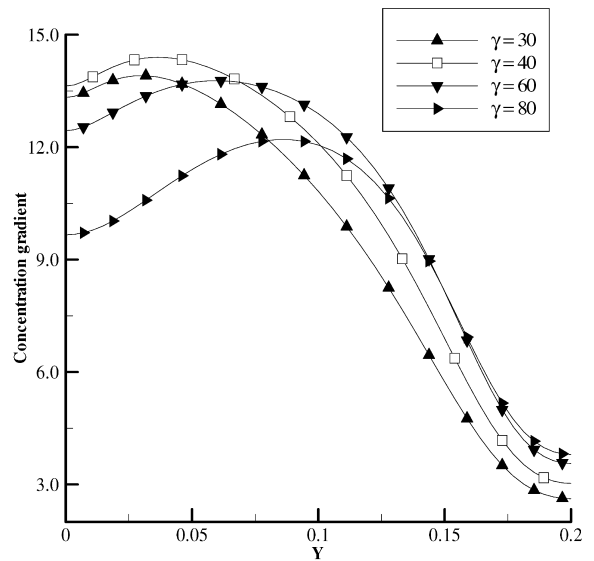
4. Summary

The concentration distribution for a quasi-steady state of solution crystal growth in a two-
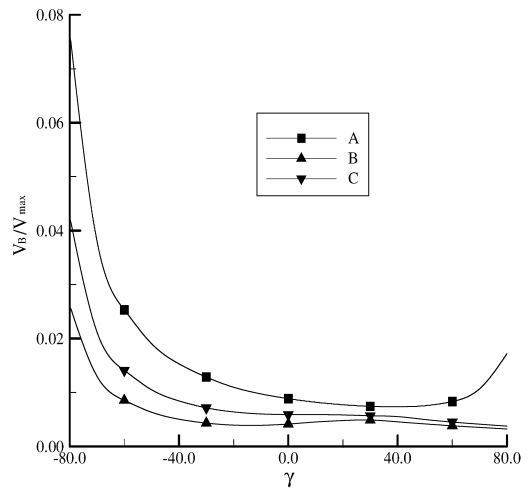
$A - \lambda = 0.2, Ra_t = 1000; B - \lambda = 0.2, Ra_t = 10000; C - \lambda = 0.4, Ra_t = 1000$

Fig. 5. Ratio of interfaces velocity to solution maximum velocity versus gravity orientation.

$\lambda = 0.2, Ra_t = 10000$

Fig. 6. Local concentration gradient $-\partial\phi/\partial X$ along the growth interface.

dimensional rectangular container in low gravity is numerically investigated in this paper. A linear diffusion-reaction theory is employed to describe the dissolution and the growth processes, and the effect

of the moving interfaces on the concentration distribution at the growth interface is considered. A comparison of this new model is made with the simple model used in previous papers [5,6], in which the dissolution process is treated as the pure diffusion process and the moving interfaces are assumed as fixed boundaries. It is shown that it is imperative to consider the effect of the moving interfaces on the supersaturation at the growth interface for some cases. For small aspect ratio and small gravity magnitude, because compared with the convection velocity the crystal growth and dissolution velocities are not small enough to neglect, except for some orientations, e.g., $0° \leqslant \gamma \leqslant 50°$ for $\lambda = 0.2$, $Ra_t = 1000$ in this work, the dissolution and the growth interfaces must be treated as the moving boundaries. For large aspect ratio or large gravity magnitude, the effect of the moving interfaces on the concentration distribution at the growth interface can be neglected except for $\gamma < -50°$. Through the comparison made in this work, a further understanding of the feasibility and the limitation of the simple treatment has been achieved.

References

[1] Z.Y. Xu, C.R. Huo, P.W. Ge, J. Crystal Growth 125 (1992) 135.

[2] Z.Y. Xu, P.W. Ge, C.R. Huo, Z.H. Zhu, J. Crystal Growth 129 (1993) 506.

[3] C.R. Huo, Z.Y. Xu, W.D. Huang, P.W. Ge, Z.H. Zhu, J. Crystal Growth 158 (1996) 359.

[4] J.C. Mullin, Crystallization, 3rd, Butterworths, London, 1993.

[5] W. Wang, W.R. Hu, J. Crystal Growth 160 (1996) 398.

[6] W. Wang, W.R. Hu, Adv. Space Res., to be published.

[7] J. Sun, F.M. Carlson, W.R. Wilcox, Simulation of TGS Crystal Growth in Space, 42nd IAF, October 5–11, 1991, Montreal, Canada.

[8] W.R. Hu, R.R. You, Acta Mech. Sin. 25 (1993) 276.

[9] H. Lin, F. Rosenberger, J.I.D. Alexander, A. Nadarajah, J. Crystal Growth 151 (1995) 153.

[10] W. Wang, W.R. Hu, Microgravity Sci. Technol., in press.

[11] P.S. Chen, Int. J. Heat Mass Transfer 22 (1979) 1669.